J|A|C|S
ARTICLES
Published on Web 08/05/2006

Periodic Density Functional Theory Study of Propane Oxidative Dehydrogenation over V_2O_5(001) Surface

Hui Fu, Zhi-Pan Liu, Zhen-Hua Li, Wen-Ning Wang,* and Kang-Nian Fan*

Contribution from the Shanghai Key Laboratory of Molecular Catalysis and Innovative Materials, Center for Theoretical Chemical Physics, Department of Chemistry, Fudan University, Shanghai, 200433, China

Received February 18, 2006; E-mail: wnwang@fudan.edu.cn; knfan@fudan.edu.cn

Abstract: The oxidative dehydrogenation (ODH) of propane on single-crystal V_2O_5(001) is studied by periodic density functional theory (DFT) calculations. The energetics and pathways for the propane to propene conversion are determined. We show that (i) the C−H bond of propane can be activated by both the terminal and the bridging lattice O atoms on the surface with similar activation energies. At the terminal O site both the radical and the oxo-insertion pathways are likely for the C−H bond activation, while only the oxo-insertion mechanism is feasible at the bridging O site. (ii) Compared to that at the terminal O site, the propene production from the propoxide at the bridging O site is much easier due to the weaker binding of propoxide at the bridging O. It is concluded that single-crystal V_2O_5(001) is not a good catalyst due to the terminal O being too active to release propene. It is expected that an efficient catalyst for the ODH reaction has to make a compromise between the ability to activate the C−H bond and the ability to release propene.

1. Introduction

With the ever-increasing worldwide demand for olefins, alternative inexpensive ways to produce light olefins in industry are highly desired.[1] As alkane is a source of inexpensive raw materials, the functionalization of light alkanes by selective oxidation has attracted considerable interest.[2] Currently, the direct dehydrogenation of alkane to olefin is a rather promising solution, although it still suffers from low yield. Compared to the conventional nonoxidative routes, the so-called oxidative dehydrogenation (ODH) has many advantages. For example, the ODH is thermodynamically favored even at low temperatures; it does not lead to the formation of coke and lower-molecular weight byproducts such as CO.

Supported vanadium oxides are one of the best catalysts for the ODH of propane[3−13] with high thermal stability and the large surface area. Several research groups have studied the mechanisms of ODH reaction on vanadium-based catalysts.[7−9] It is established that the ODH reaction on supported vanadium catalysts proceeds via a Mars−van Krevelen mechanism [14,15] and the C−H bond activation step is the rate-determining step.[16−19] The reaction mechanism can be described as (i) the reduction of the oxide surface by hydrocarbon and (ii) the subsequent reoxidation by the gas-phase oxygen. It was also found that the propane conversion and the propene selectivity is often inversely related.[20,21] Generally, the activity and selectivity of the catalyst depends on its reducibility and basicity.[22] To achieve high activity and selectivity the presence of highly dispersed vanadium is crucial.[23,24] It is found that at low loadings vanadium is molecularly dispersed, whereas at higher loadings V_2O_5 crystallites start to appear.[25−31]

To understand the mechanism of the ODH reaction, it is crucial to know where the reaction occurs. Generally, there are three types of lattice oxygens on vanadium surfaces. (i) Singly coordinated terminal oxygen, O(1), which is a vanadyl oxygen (V═O); (ii) two-coordinated oxygen, O(2); and (iii) three-coordinated oxygen, O(3). The O(2) and O(3) bridge two and three vanadium atoms, respectively. To date, it remains controversial what kind of oxygens are responsible for the propane ODH. We have classified the literature according to the suggested active O species, which are reviewed briefly in the following.

(1) Cavani, F.; Trifiro, F. *Catal. Today* **1995**, *24*, 307.
(2) Centi, G.; Cavani, F.; Trifiro, F. *Selective Oxidation by Heterogeneous Catalysis*; Kluwer Academic/Plenum: New York, 2001.
(3) Chaar, M. A.; Patel, D.; Kung, H. H. *J. Catal.* **1988**, *109*, 463.
(4) Corma, A.; Lopez Nieto, J. M.; Paredes, N. *J. Catal.* **1993**, *144*, 425.
(5) Hardcastle, F. D.; Wachs, I. E. *J. Mol. Catal.* **1988**, *46*, 173.
(6) Deo, G.; Wachs, I. E.; Haber, J. *Crit. Rev. Surf. Chem.* **1994**, *4* (3/4), 141.
(7) Wachs, I. E.; Wechuysen, B. M. *Appl. Catal., A* **1997**, *157*, 67.
(8) Eon, J. G.; Olier, R.; Volta, J. C. *J. Catal.* **1994**, *145*, 318.
(9) Balsko, T.; Lopez Nieto, J. M. *Appl. Catal., A* **1997**, *157*, 117.
(10) Khodakov, A.; Olthof, B.; Bell, A. T.; Iglesia, E. *J. Catal.* **1999**, *181*, 205.
(11) Khodakov, A.; Yang, J.; Su, S.; Iglesia, E.; Bell, A. T. *J. Catal.* **1998**, *177*, 343.
(12) Kondratenko, E. V.; Baerns, M. *Appl. Catal., A* **2001**, *222*, 133.
(13) Argyle, M. D.; Chen, K.; Iglesia, E.; Bell, A. T. *J. Catal.* **2002**, *208*, 139.
(14) Creaser, D.; Andersson, B.; Hudgins, R. R.; Silveston, P. L. *Appl. Catal., A* **1999**, *187*, 147.
(15) Mamedov, E. A.; Cortés Corberán, V. *Appl. Catal., A* **1995**, *127*, 1.
(16) Chen, K. D.; Khodakov, A.; Yang, J.; Iglesia, E. *J. Catal.* **1999**, *186*, 325.
(17) Andersen, P. J.; Kung, H. H. *J. Phys. Chem.* **1992**, *96*, 318.
(18) Burch, R.; Swarnakar, R. *Appl. Catal.* **1991**, *70*, 129.
(19) Chen, K.; Iglesia, E.; Bell, A. T. *J. Catal.* **2000**, *192*, 197.
(20) Kung, H. H. *Adv. Catal.* **1994**, *40*, 1.
(21) Albonetti, S.; Cavani, F.; Trifiro, F. *Catal. Rev.—Sci. Eng.* **1996**, *38*, 413.
(22) Chen, K.; Bell, A. T.; Iglesia, E. *J. Phys. Chem. B* **2000**, *104*, 1292.
(23) Bond, G. C.; Bruckman, K. *Faraday Discuss. Chem. Soc.* **1989**, *72*, 235.
(24) Bosch, H.; Hanssen, F. *Catal. Today* **1986**, *2*, 369
(25) Roozeboom, F.; Mittelmeijer-Hazeleger, M.; Moujlin, J.; Medema, J.; de Beer, V.; Gellings, P. *J. Phys. Chem.* **1990**, *84*, 2783.
(26) Wachs, I.; Saleh, R.; Chan, S.; Cherisch, C. *Appl. Catal.* **1985**, *15*, 339.
(27) Went, G.; Oyama, T.; Bell, A. T. *J. Phys. Chem.* **1990**, *94*, 4240.
(28) Eckert, H.; Wachs, I. *J. Phys. Chem.* **1989**, *93*, 6976.
(29) Deo, G.; Eckert, H.; Wachs, I. *Am. Chem. Soc.* **1990**, 16. 112, 9017.
(30) Kozlwoski, R.; Pettifer, R.; Thomas, J. *J. Phys. Chem.* **1983**, *87*, 5176.
(31) Haber, J.; Kozlowska, A.; Kozlwoski, R. *J. Catal.* **1986**, *102*, 52.

10.1021/ja0611745 CCC: $33.50

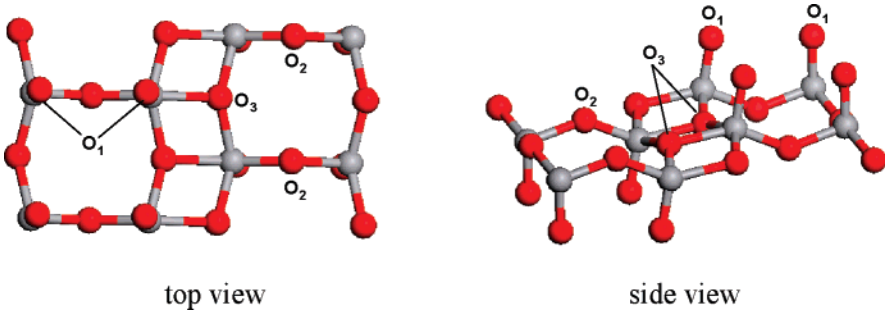

Figure 1. The unit cell of $V_2O_5(001)$ surface.

O(1) is suggested to be the active species as early as 1968 since Tarama et al. found the key role of the O(1) atoms by studying the adsorption on the V_2O_5 surface using IR spectroscopy.[32] The oxidation of butane on unsupported and supported V_2O_5 catalysts were investigated by Mori et al.[33] It was found that the reaction rate at a given O_2 concentration was in proportion to the amount of V^{5+}═O species in the catalyst, indicating that the surface V═O is the reaction site for the reaction. By studying the oxidation reaction of ethane on a series of well-characterized samples of silica-supported vanadium oxide, Oyama and co-workers[34] suggested that singly coordinated vanadyl oxygen O(1) may be the active center. Theoretically, Andersson[35] calculated the electronic structure of V_2O_5 using empirical formula, and suggested that the V═O species on the surfaces are responsible for the catalytic oxidation of hydrocarbons. Recently, Gilardoni et al.[36] investigated the ODH reaction of propane on a small V_2O_5 cluster ($V_4O_{14}H_8$) by DFT, and the O(1) is found to be more active (Fukui function).

On the other hand, the possibility of O(2) participating in the catalytic process was also reported. Eon et al.[8] proposed that the bridging oxygen atoms were the active sites for catalytic oxidation of propane on γ-Al_2O_3-supported V_2O_5 by ESR, NMR, and Raman spectrocopies. A recent atomic force microscopy (AFM) study of the $V_2O_5(001)$ surface[37] suggested the O(2) as the active site. Sambeth et al.[38] studied the catalytic oxidation of CH_3OH to CH_3COOH on the V_2O_5 surface by cluster calculations. Their results indicated that the bridging oxygens might participate in nucleophilic oxidation process of organic molecules. Hartree−Fock and DFT calculations on small VO_x clusters by Witko and co-workers[39] suggested that the H atoms bond preferentially with the O(2). Kamper et al.[40,41] calculated the physisorption of propane and ethane on $V_2O_5(001)$ surface by molecular mechanics. They found that the physisorption of propane at the O(2) site was the most stable and thus might be the precursor for the subsequent catalytic reaction.

Compared to O(1) and O(2), very few studies suggested O(3) to be the active center. Nevertheless, using semiempirical calculations, Ramirez et al.[42] found that the O-vacancy left at the O(3) site was the most stable compared to that at the O(1) and the O(2) site.

In an aim to gain a deeper insight into the ODH mechanism, here we have studied the conversion of propane to propene on $V_2O_5(001)$. In particular, the catalytic roles of different surface O species are investigated in detail. $V_2O_5(001)$ is selected as the model catalyst since $V_2O_5(001)$ is the most stable surface exposed in crystalline V_2O_5, and experimental studies also suggested that the mechanism of propane ODH on bulk V_2O_5 is the same as that on supported vanadium catalyst.[16] V_2O_5 crystal (*Pmmn*59) exhibits a layered structure along the ⟨001⟩ direction with weak van der Waals interaction between layers. Previous experimental[43] and theoretical[44,45] studies have demonstrated that the (001) surface has very similar physical properties and stability to those of the bulk crystal. Therefore, the reaction picture we obtained on $V_2O_5(001)$ can pave the way toward the clarification of the activity of supported vanadium catalysts and better catalyst design.

2. Computational Details

All total energy density functional theory calculations were carried out with VASP package using plane wave basis sets.[46,47] The exchange-correlation functional utilized is the local-density-approximation with generalized gradient correction, known as GGA-PW91.[48,49] The kinetic cut-off energy used is 400 eV. The valence electrons of elements are treated by Vanderbilt ultrasoft pseudopotentials.[50,51] The 3p, 3d, and 4s states (11 electrons) of V states are treated as valence states to guarantee a good transferability of the V potential. The Monkhorst−Pack Brillouin-zone (BZ) sampling is used with $0.05 \times 2\pi$ (1/Å) spacing in reciprocal space.[52] For example, for a (1×2) surface unit cell of $V_2O_5(001)$ a (2×3) k-point grid is adopted (Figure 1). Spin-polarization has been considered during calculations, and it was found to be important for radical-containing systems.

Without specific mentioning, the $V_2O_5(001)$ surface is routinely modeled by a one-layer slab with all the atoms allowed to relax. The vacuum region between slabs is ∼10 Å. The structure of $V_2O_5(001)$ is shown in Figure 1. The one-layer model is justified because V_2O_5 bulk has a layered structure, with the layer−layer bonding belonging to van der Waals interaction.[43] For the C−H bond activation reactions, our

(32) Tarama, K.; Yoshida, S.; Ishida, S.; Kakioka, H. *Bull. Chem. Soc. Jpn.* **1968**, *41*, 2840.
(33) Mori, K.; Miyamoto, A.; Murakami, Y. *J. Phys. Chem.* **1985**, *89*, 4265.
(34) Oyama, S. T. *J. Catal.* **1991**, *128*, 210.
(35) Andersson, A. *J. Solid State Chem.* **1982**, *42*, 263.
(36) Gilardoni, F.; Bell, A. T.; Chakraborty, A.; Boulet, P. *J. Phys. Chem. B* **2000**, *104*, 12250.
(37) Costa, A. D.; Mathieu, C.; Barbaux, Y.; Poelman, H.; Dalmai-Vennik, G.; Fiermans, L. *Surf. Sci.* **1997**, *370*, 339.
(38) Sambeth, J.; Juan, A.; Gambaro, L.; Thomas, H. *J. Mol. Catal. A: Chem.* **1997**, *118*, 283.
(39) Witko, M.; Hermann, K.; Tokrarz, R. *Catal. Today.* **1998**, *50*, 553.
(40) Kamper, A.; Auroux, A.; Baerns, M. *Phys. Chem. Chem. Phys.* **2000**, *2*, 1069.
(41) Kamper, A.; Hahndorf, I.; Baerns, M. *Top. Catal.* **2000**, *11*, 77.
(42) Ramirez, R.; Casal, B.; Utrera, L.; Ruiz-Hitzky, E. *J. Phys. Chem.* **1990**, *94*, 8960.
(43) Poelman, H.; Vennik, J.; Dalmai, G. *J. Electron Spectrosc. Relat. Phenom.* **1987**, *44*, 251.
(44) Yin, X.; Fahmi, A.; Endou, A.; Miura, R.; Gunji, I.; Yamauchi, R.; Kubo, M.; Chatterjee, A.; Miyamoto, A. *Appl. Surf. Sci.* **1998**, *130*, 539.
(45) Lambrecht, W.; Djafari-Rouhani, B.; Vennik, J. *J. Phys. C* **1981**, *14*, 4775.
(46) Kresse, G.; Hafner, J. *Phys. Rev. B* **1993**, *47*, 558.
(47) Kresse, G.; Hafner, J. *Phys. Rev. B* **1994**, *49*, 14251.
(48) Perdew, J. P.; Chevary, J. A.; Vosko, S. H.; Jackson, K. A.; Penderson, M. R.; Singh, D. J.; Fiolhais, C. *Phys. Rev. B* **1992**, *46*, 6671.
(49) Perdew, J. P.; Wang, Y. *Phys. Rev. B* **1992**, *45*, 13244.
(50) Kresse, G.; Hafner, J. *J. Phys.: Condens. Matter* **1994**, *6*, 8245.
(51) Vanderbilt, D. *Phys. Rev. B* **1990**, *41*, 7892.
(52) Monkhorst, H. J.; Pack, J. D. *Phys. Rev. B* **1976**, *13*, 5188.

test calculations with bilayer slabs show essentially the same result (both in V−O bond length and atomic charges) as that from a monolayer slab calculation. The multilayer calculations are only necessary when the surface is largely disturbed, for example, O vacancy formation.

The adsorption energy (E_{ads}) was calculated according to the expression

$$E_{ads} = E(_{adsorbate-substrate}) - (E_{adsorbate} + E_{substrate})$$

where E_X is the DFT-total energy of the X system. A negative E_{ads} indicates the adsorption will gain energy.

Transition states (TS) were searched with the "climbing-images" nudged elastic band (CI-NEB) algorithm.[53,54] A total of eight images from the linear interpolation between the reactant and product states are used as the initial guesses for the reaction coordinates. The individual images are then optimized with the NEB algorithm (a constrained molecular dynamics algorithm). To obtain a better resolution of the minimum energy path in the vicinity of the transition state, the images next to the transition state are extrapolated along the potential energy surface (PES) to locate the saddle point. The reaction barrier is determined as the energy difference between the saddle point and the initial state. It might be mentioned that in transition state theory it is ΔH that enters into the rate equation. However, we noticed that the difference between E_a and ΔH is normally small and will not change the chemistry revealed in the work. For example, for the reaction barrier of a C−H bond breaking, the E_a and ΔH is different by <4 kcal/mol at temperatures such as 800 K (from our cluster-model calculations according to ref 55).

3. Results and Analysis

3.1. Molecular Adsorption of Propane. Molecular adsorption of ethane and propane on both the perfect and the defective (O−Vacancy) V_2O_5(001) surface have been studied by Kamper et al.[40,41] using the molecular mechanics method. On the perfect V_2O_5(001) surface, the potential energy surface of the adsorption is found to be quite flat. The most favorable adsorption sites for ethane and propane are near the O(2) site between the two double rows of O(1), while the adsorption is the weakest near the O(1) site. At the O(2) site the adsorption energies are calculated to be ∼−8 kcal/mol for propane and −5.6 kcal/mol for ethane. By contrast, a DFT-cluster study by Gilardoni et al.[36] found no evidence of propane adsorption near the two adjacent vanadyl oxygens (O(1)) on the V_2O_5 cluster.

On the basis of the DFT-slab model, we have examined the molecular adsorption of propane at various oxygen sites on V_2O_5(001). Geometry optimization has been performed starting from propane at different guessed orientations near the O(1), O(2), and O(3) sites. Several possible adsorption states at each O site are located by varying the conformation of propane, and their differences in energy are very small (<2 kcal/mol). Although the most stable structure is found to be at the O(2) site, consistent with that reported,[40] it turns out that propane could not adsorb on the surface with all the adsorption energies at three sites being positive (1.57 kcal/mol O(1), 0.30kcal/mol O(2), and 2.13 kcal/mol O(3)). It should be noted that the GGA functional in DFT mainly describes the electrostatic interaction part of van der Waals interaction and thus leads to an underestimation of physisorption energy (the magnitude is not large, usually below 5 kcal/mol). The above results show that propane does not form a molecular adsorption state on the surface or only physisorbs on V_2O_5(001) very weakly. Considering that the ODH reaction occurs at high temperatures, e.g., ∼800 K, the propane in the gas phase can easily be more stable (Gibbs free energy) than it is on the surface due to the large entropy contribution of the gas-phase molecule. It is thus expected that the C−H bond breaking of propane over V_2O_5(001) is not precursor mediated but belongs to a direct dissociation.

3.2. C−H Bond Activation. The breaking of a propane C−H bond can occur in the methyl or the methylene groups of propane, and the product is *n*-propoxide or *i*-propoxide species on the surface, respectively. It is known from thermodynamics that the C−H bond energy in the methyl group is stronger than that in the methylene group (420 kJ/mol and 401 kJ/mol, respectively). Experimentally, isotopic studies by Chen et al.[19] found the similar primary dehydrogenation rates for $CH_3CD_2CH_3$ and $CD_3CD_2CD_3$, which indicates that only the methylene C−H bond is involved in the rate-determining step. The theoretical study by Gilardoni et al.[36] also showed that the formation of *i*-propoxide is both thermodynamically and kinetically favored. Thus, in this work we have focused on the C−H bond activation leading to *i*-propoxide formation.

As for how the C−H bond breaks in metal oxides, there are two different ways that have been proposed.[56] The first one is heterolytic splitting, leading to an alkyl anion and a proton. This is usually present on the surface with strong acid−base pairs. Another one is homolytic cleavage that usually takes place at surface oxygen sites. In the isotopic labeling studies[16,19] by Chen et al., the C−H bond activation was suggested to follow two steps: (i) Propane dissociatively adsorbs on the surface to form a propoxide and a hydroxyl group, which consumes two lattice oxygen atoms. (ii) The propoxide then releases a H atom to a third lattice oxygen atom to produce propene. In this two-step mechanism, the C−H bond undergoes homolytic splitting, and the reaction center is purely lattice oxygen without involving the vanadium atom.

To provide a deeper insight, we have calculated the heterolytic cleavage of the C−H bond at a terminal O(1) site; two reaction paths are considered.

$$C_3H_7{-}H + V{=}O \leftrightarrow HV{=}OC_3H_7 \quad (1)$$

$$C_3H_7{-}H + V{=}O \leftrightarrow C_3H_7V{=}OH \quad (2)$$

In process 1, the propyl group and the H atom bind with the terminal oxygen and the vanadium, respectively. The heterolytic cleavage of C−H bond results in a negatively charged H atom. The transition state of the reaction has been located, and the reaction barrier is calculated to be 80.7 kcal/mol. With such a high activation barrier, it is expected that this reaction path is unlikely to account for the activity of propane ODH occurring at 800 K.[19] For process 2, we have not been able to locate the proposed final state, $C_3H_7V{=}OH$, including the V cations with the V=O pivoting either inward or outward on the surface (Figure 1). From our calculations, the adsorbed propyl group on the V atom is not stable at the V=O site. Overall, the heterolytic cleavage of the C−H bond for activation of propane over the V_2O_5(001) surface can be ruled out, which agrees with the general consensus since no strong acid−base pairs exist on V_2O_5(001).

(53) Henkelman, G.; Uberuaga, B. P.; Jönsson, H. *J. Chem. Phys.* **2000**, *113*, 9901.
(54) Henkelman, G.; Jönsson, H. *J. Chem. Phys.* **2000**, *113*, 9978.
(55) Fu, G.; Xu, X.; Lu, X.; Wan, H. *J. Phys. Chem. B* **2005**, *109*, 6416
(56) Martin, G. A.; Mirodatos, C. *Fuel Process Technol.* **1995**, *42*, 179.

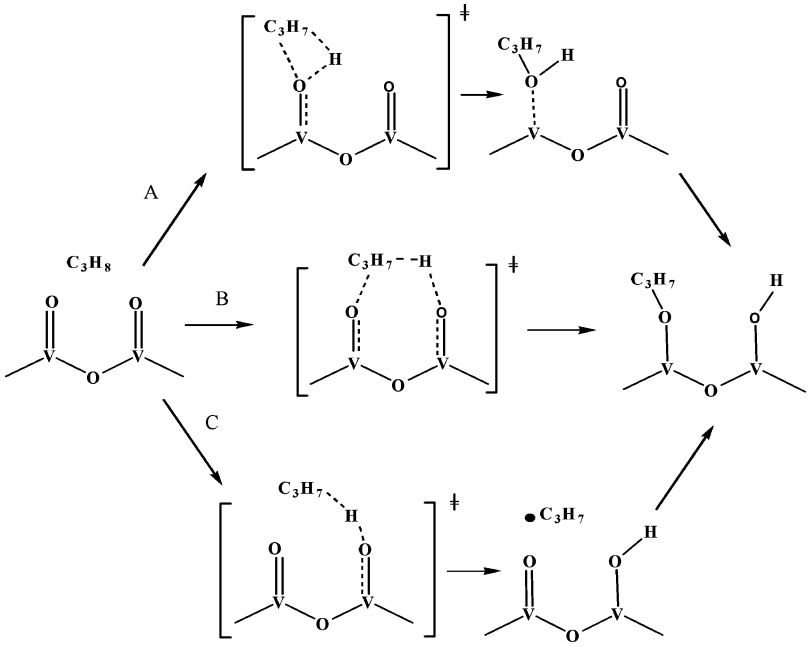

Figure 2. Three homolytic cleavage mechanisms for the C−H bond activation of propane.

For the homolytic cleavage, the chemical reaction can be represented as

$$C_3H_7{-}H + O + O \leftrightarrow C_3H_7O + HO \qquad (3)$$

Because of two lattice O atoms involved, a great complexity is encountered in considering the reaction occurring on V_2O_5(001). With three different lattice O's available on the V_2O_5(001) surface, nine combinations in total are possible for the reaction path, i.e. O(1)−O(1), O(1)−O(2), O(1)−O(3), O(2)−O(1), O(2)−O(2), O(2)−O(3), O(3)−O(1), O(3)−O(2), and O(3)−O(3). Furthermore, for every O−O combination, we considered three possible mechanisms, namely, oxo-insertion mechanism (A), concerted mechanism (B), and radical mechanism (C) (Figure 2).

Mechanism A. A lattice oxygen atom inserts into the C−H bond of the propane to form an alcoholic intermediate on the surface. The proton of the alcoholic intermediate is then transferred to another lattice oxygen nearby.

Mechanism B. In one step, the propane reacts with two adjacent oxygen atoms on the surface in a concerted way. This path features a ring TS.

Mechanism C. A lattice oxygen atom abstracts a H atom from propane directly to leave a propyl radical in the gas phase. It is then followed by the rebound of the propyl radical to a second surface oxygen.

In short, the various C−H bond activation pathways can be denoted as O(m)−O(n)-X, where m, n = 1, 2, 3 and X = A, B, C mechanisms. The first O, O(m), denotes the O site where a propane attacks the surface initially. We will go through our DFT results for these pathways in the following subsections.

3.2.1. O(1) site: O(1)−O(n)-X. (a) O(1)−O(n)-A. In the O(1)−O(1)-A pathway, the C−H bond is activated via a transition state TS1 (shown in Figure 3) by inserting the lattice O into the C−H bond. At the TS1, the C−H bond elongated from 1.10 to 2.09 Å, and the distance between the C atom of propane and the O(1) atom is shortened to 2.76 Å. At the same time, the OH group is nearly formed with the O−H bond being

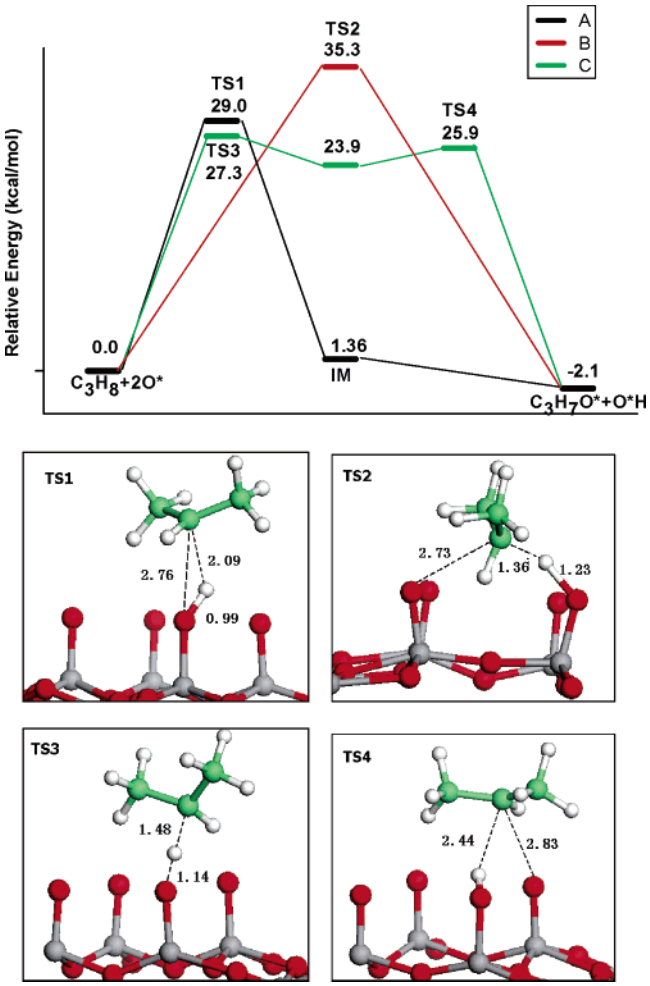

Figure 3. Energy profile of C−H bond activation at the O(1) site and the structures of related transition states.

0.99 Å. The calculated energy barrier is 29.0 kcal/mol. The obtained alcoholic-like intermediate is 1.36 kcal/mol less stable than the initial state. In this intermediate, the C−O and O−H

bonds are already formed ($d_{C-O(1)}$ = 1.49 Å, $d_{H-O(1)}$ = 1.06 Å), and the C−H bond is nearly broken with a bond length of 2.09 Å. The bond length of V═O is elongated by 0.32 Å. The following step of H atom migration to the adjacent O(1) atom is a barrierless process. In the final state, the bond lengths of C−O and O−H of *i*-propoxide are 1.45 Å and 0.98 Å, respectively. This path was also studied by Gilardoni et al.[36] with a cluster model, and a much smaller energy barrier (9.4 kcal/mol) was predicted.

The O(1)−O(2)-A and O(1)−O(3)-A pathways differ from the O(1)−O(1)-A pathway only in the step of H atom migration. In these pathways, the H atom migrates to the O(2) and the O(3) sites, respectively. By calculating the H atom binding on the O(2) and the O(3) site, we have found that the H atom at the O(2) and the O(3) sites are less stable by 7.2 kcal/mol and 0.63 kcal/mol, respectively, than it at the O(1) site The reaction barrier of the H migration in the O(1)−O(2)-A is calculated to be 5.4 kcal/mol, while the transition state of H migration in the O(1)−O(3)-A cannot be located with the NEB method. Comparing the three O(1)−O(*n*)-A pathways, we found that the H migration ability is related to the stability of the H atom on various lattice oxygen atoms. Because a H−O(1) binding is much stronger, the O(1) site should always be preferred at this step. To sum up, in the O(1)−O(*n*)-A groups, the O(1)−O(1)-A is the lowest-energy pathway, in which the C−H bond breaking to form an alcoholic intermediate is the most difficult step with a barrier of 29.0 kcal/mol.

(b) O(1)−O(*n*)-B. In the concerted mechanism, a ring TS (TS2) can be easily achieved on two neighboring O(1) atoms with the reaction barrier of 35.3 kcal/mol. The structure of the TS2 is depicted in Figure 3, where the distance between propyl and O(1) atom is 2.73 Å and the forming H−O bond is 1.23 Å. For O(1)−O(2)-B, the located TS structure is not a ring structure but more like a TS belonging to a radical mechanism, and the obtained reaction barrier is quite high (47.1 kcal/mol). As for O(1)−O(3)-B, the energy barrier is even higher, 20.0 kcal/mol higher than that in O(1)−O(1)-B. Overall, the O(1)−O(1)-B pathway is less favorable compared to the O(1)−O(1)-A.

(c) O(1)−O(*n*)-C. In the radical mechanism C, all the three O(1)−O(*n*)-C share the same initial step, namely, the H abstraction by the O(1). The TS of this step has been located (TS3 in Figure 3), and the reaction barrier is calculated to be 27.3 kcal/mol. At the TS, the C−H bond is lengthened to 1.48 Å, and the H−O distance is only 1.14 Å. After the TS, a propyl radical is formed in the gas phase. At the next step, the propyl radical adsorbs on the lattice oxygens. We found that the nearest O(1) site is the most favored site and the reaction has a very small reaction barrier (2.0 kcal/mol). For the propyl radical migrating to the O(2) site, the reaction barrier is 9.3 kcal/mol. However, for the propyl radical migrating to the O(3) site, the final state structure is less stable than that on O(1) and deformed so much that one of the V−O bonds has been ruptured, leading to two coordinated O's. Thus, they cannot compete with that occurring on the O(1) site. It is noticed that the activation energy along the O(1)−O(1)-C (27.3 kcal/mol) is slightly lower than that in the O(1)−O(1)-A, indicating that the radical mechanism is the best among the O(1)−O(*n*)-X pathways.

To verify the preference of breaking methylene C−H bond over methyl C−H bond, we calculated the energy barrier of methyl C−H bond activation through mechanism C. The

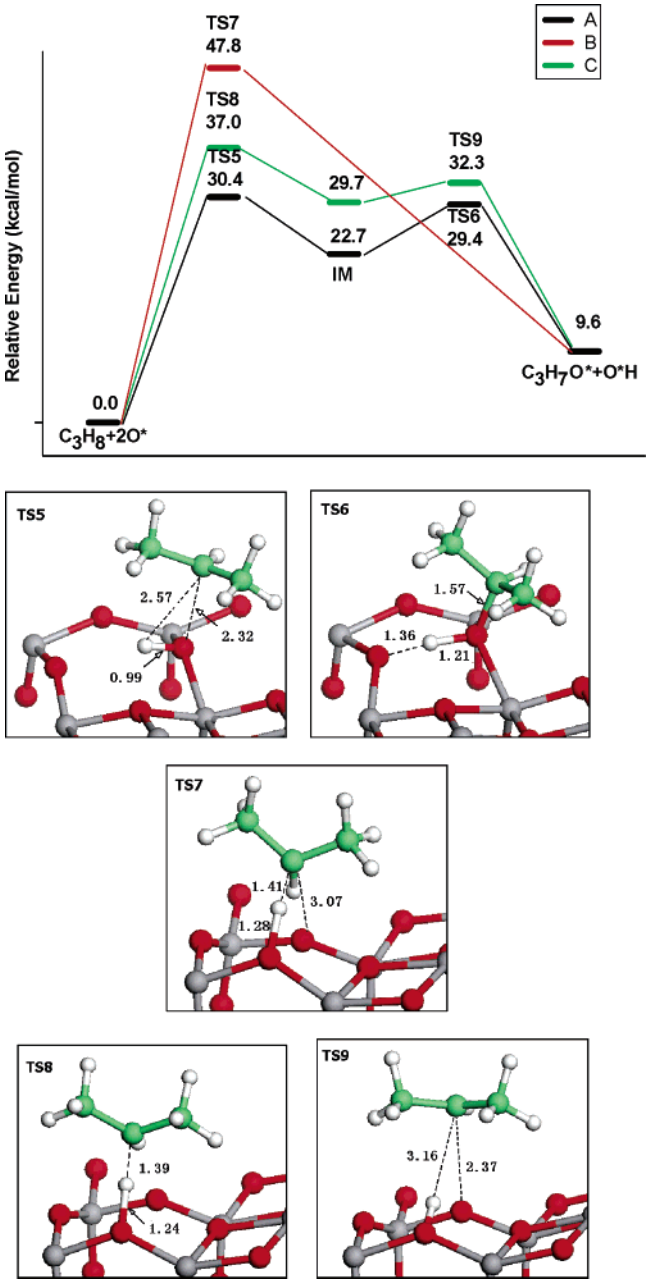

Figure 4. Energy profiles of C−H bond activation at the O(2) site and structures of related transition states.

calculation result predicts an energy barrier of 7.3 kcal/mol higher than that of methylene C−H bond breaking, which is consistent with previous experimental and theoretical studies.[19,36] In the following sections, the possibility of methyl C−H bond activation is not considered any more.

3.2.2. O(2) Site: O(2)−O(*n*)-X. The pathways of the O(2)−O(*n*)-X are similar to their O(1)−O(*n*)-X counterparts, and here we will mainly concentrate on their differences. Unlike the situation on the O(1) sites where O(1)−O(1)-C is the lowest-energy pathway, the energetically most favored pathway on the O(2) site is found to be O(2)−O(2)-A. The energy profile of this pathway and the related TSs are shown in Figure 4. The O(2)−O(1)-A and O(2)−O(3)-A can be excluded because (i) the reaction barrier of the H migration to the O(1) site is higher than that to the O(2) due to the larger distance between the O(2) and the O(1), and (ii) the binding of H atom with the O(3) is

Table 1. Bader Charge Difference of the Atoms in the System on Going from the Initial State (Propane in the Gas Phase Plus the Clean Surface) to the Transition States (TSs) and to the Intermediate States (IMs) in the C−H Bond Activation[a]

	IMs				TSs			
	O(1)–A	O(2)–A	O(1)–C	O(2)–C	O(1)–A	O(2)–A	O(1)–C	O(2)–C
O(1)[b]	−0.84		−0.80		−0.77		−0.25	
O(2)[b]		−0.53		−0.60		−0.58		−0.06
V	−0.05	−0.14	−0.07	−0.10	−0.05	−0.11	−0.07	−0.07
	−0.10	−0.12	−0.05	−0.04	−0.04	−0.09	−0.07	−0.03
	−0.03	−0.07	−0.04	−0.04	−0.03	−0.06	−0.05	−0.03
	−0.05	−0.05	−0.04	−0.03	−0.02	−0.06	−0.04	−0.06
	−0.03	−0.05	−0.04	−0.02	−0.00	−0.05	−0.04	−0.04
	−0.03	−0.04	−0.03	−0.01	−0.00	−0.04	−0.02	−0.01
	0.00	−0.03	−0.02	−0.01	0.03	−0.03	−0.01	−0.03
	0.01	−0.02	0.02	−0.00	0.03	−0.03	−0.00	−0.00
V_{sum}[c]	−0.27	−0.52	−0.28	−0.27	−0.10	−0.49	−0.30	−0.28
O_{sum}[d]	−0.47	−0.55	−0.13	−0.40	−0.40	−0.53	−0.06	−0.17
C_3H_8	1.59	1.60	1.21	1.27	1.26	1.59	0.61	0.51
net spin (μ_B)	2.06	2.04	2.08	2.07	2.08	2.04	1.46	1.55

[a] Negative value means electron gain. The net spin of each state is also listed. The unit of charge is $|e|$. [b] The reacting oxygen atoms in the unit cell. [c] Sum of the net charges on all the V atoms in a unit cell. [d] Sum of the net charges on all O atoms in a unit cell except the reacting O atom.

the weakest on the surface. As for the other possibilities, O(2)−O(*n*)−B and O(2)−O(*n*)-C, these pathways have much higher reaction barriers than that in O(2)−O(2)-A. The activation energy of O(2)−O(*n*)-C is about 6.3 kcal/mol higher than O(2)−O(2)-A, while the barrier in O(2)−O(*n*)-B is even higher (47.3 kcal/mol).

From Figure 4, it can be seen that the process of forming *i*-propoxide on the O(2) site will cost 9.6 kcal/mol. The lowest possible activation energy is 30.4 kcal/mol, which is comparable to the 27.3 kcal/mol on the O(1) site. The intermediate complex in the O(2)−O(2)-A is very unstable compared to its counterpart in the O(1)−O(1)-A (Figure 3). Therefore, compared to the pathways on the O(1) site, the dissociative adsorption on the O(2) site is unfavorable in thermodynamics, but it is competitive in kinetics.

3.2.3. O(3) Site: O(3)−O(*n*)-X. The C−H bond activation on the O(3) site is the least possible, apparently because the O(3) is three-fold coordinated and thus the most inert, as also reported in previous literature.[57] Thermodynamically, the adsorption states related to the O(3) sites are generally unstable. For instance, in mechanism A, the stability of the intermediates decreases drastically from O(1) to O(2) and to O(3), with the relative energies being 1.4, 22.7, and 31.8 kcal/mol, respectively. Furthermore, the adsorption of propyl group on O(3) can induce strong surface reconstruction by breaking one of the O(3)−V bonds, which makes the propyl adsorption on the O(3) the least stable. For the A and B mechanisms, we have located the TSs for the O(3)−O(1)-A and O(3)−O(3)-B. These two pathways exhibit high reaction barriers, i.e., 47.0 and 41.0 kcal/mol, respectively. The C mechanism (O(3)−O(*n*)−C pathways) is unlikely as well, since O(3) is less active than the O(2) and the O(1) sites according to the intermediate state stability. Therefore, the possibility of the three-fold coordinated O(3) as the reaction center of propane activation can be ruled out.

3.2.4. Electronic Structure Analysis. From the above results, we found that the activation of the C−H bond does not show strong preference to the O(1) site. The reaction barrier in the pathway of the O(1) site is only 3.1 kcal/mol (= 30.4 − 27.3) lower than that of the O(2) site. To understand this, we have first computed the atomic charges of the surface atoms using the Bader charge analysis.[58] It is found that the net charge of the lattice oxygen atoms on the clean surface are −0.59, −0.93 and −1.05 $|e|$ for the O(1), O(2), and O (3), respectively. The charge distribution reflects the ability of the lattice O's to further gain electrons (reducibility). Obviously, the reducibility is the largest on O(1) while lowest on O(3). Additionally, the local bonding ability of the lattice oxygen atoms has been measured using an H atom as the probe. The H−O bonding is measured by the adsorption energy of the H atom, which shows a sequence of H−O(3) < H−O(2) < H−O(1) (−4.4 < −7.6 < −12.7 kcal/mol, referred to 1/2 H_2). Previous study also shows the same sequence.[59,60] These results indicate that the three-folded O(3) is the most negatively charged and is the most difficult to be reduced. By contrast, the O(1) atom is the most active with the strongest eletrophilic tendency.

However, the above picture does not explain the activity of the O(2). We then turn to the reaction intermediates, including the transition states, of the C−H bond activation process, which should reflect the activity difference between O(1) and O(2). The atomic charge of the intermediate states in mechanisms A and C have been calculated. Listed in Table 1 is the *change* of the Bader atomic charge of selected atoms (entities) on going from the IS, i.e., the propane in the gas phase plus the clean (001) surface, to the transition state and the intermediate states (IMs). It should be mentioned that all the states are spin-polarized, and the net spin is also listed in Table 1. Our Bader spin-charge analysis showed that the net spins are mainly located on the V's that directly link with the reacting lattice O's, while the other V's on the surface also obtain a small fraction of net spin moments.

At the intermediate states, the total net charges on C_3H_8 are +1.59, +1.21, +1.60, and +1.27 for the A and C mechanisms on the O(1) and O(2) sites, respectively. It is clear that electrons are transferred from propane to the surface. The O(1) can gain more electrons than the O(2), consistent with the above analysis. The electron transfer in the A mechanism is indeed larger than that in the C mechanism (e.g. 1.59 > 1.21), as expected from the two-electron reduction in the A mechanism and the one-electron reduction in the C mechanism, although the values are

(57) Fahmi, A.; Minot, C. *Surf. Sci.* **1994**, *304*, 343.
(58) Bader, R. F. W. *Atoms in Molecules: A Quantum Theory*; Clarendon: Oxford, 1990.
(59) Calatayud, M.; Minot, C. *J. Phys. Chem. B* **2004,** *108*, 15679.
(60) Yin, X.; Han, H.; Endou, A.; Kubo, M.; Teraishi, K.; Chatterjee, A.; Miyamoto, A. *J. Phys. Chem. B* **1999**, *103*, 1263.

not exactly two or one. It should be emphasized that the reacting O(1) or O(2) atom is the most reduced (the largest increase of negative charge) species while the charge on V atoms is not much changed compared to that at the clean surface. Considering that there is strong spin-localization on V, which is mainly due to d-states, we can expect that the original V−O d−p covalent bonding is weakened and yields nonbonding spin-polarized d states on V.

We noticed that, although the O(2) has less ability to be reduced compared to the O(1), the surface V atoms and other nonreacting O atoms can help to accommodate electrons for CH bond breaking at the O(2) site. On the basis of this charge delocalization, we can understand the activity of the O(2) site as follows. Compared to the O(1) atom, the O(2) atom has a better contact with other surface atoms: the O(2) has two V's as first neighbors, and it sits at the four-coordination bonding plane of V, while the O(1) only bonds directly with one V, and it is outside the four-coordination bonding plane. Although the O(2) itself has a lower ability to accommodate extra electrons than the O(1), the electrons at the O(2) site can be well delocalized into the nearby atoms, particularly vanadium atoms through the orbital overlap. This can help to stabilize the transition states.

Knowing the electronic structures of the O(1) and O(2), we can also rationalize their preferences for the different C−H bond activation mechanisms. At the O(1) site, mechanisms A and C can proceed with comparable activation energies, while at the O(2) site mechanism A is the only choice. From the chemical formula, it is easy to know that in the radical mechanism, C, only one electron from the H is transferred to the lattice O initially to form OH, while in the oxo-insertion mechanism, A, two electrons from a C−H bond are injected to the surface in one step. This indicates that the mechanism A, compared to the mechanism C, requires a catalyst with higher reducibility, while in the mechanism C the H−O bonding strength is more important. Therefore, for the O(2) site that has a weaker H−O(2) bonding ability but a fairly good reducibility, mechanism A is selected. Our results showed that the electron delocalization does contribute to enhance the reducibility of the surface O atoms such as the O(2).

It is of interest to compare our results with the recent DFT-cluster study of C−H bond activation over Mo_3O_9 by Fu et al. They found that the radical mechanism is far better than other mechanisms for both methane[55] and propane[61] activations. However, our current DFT-slab study shows that the oxo-insertion mechanism on the O(2) site is equivalently likely. The strong preference for the radical mechanism in their cluster calculations may be due to the finite cluster size where the long-range electron delocalization is largely suppressed.

3.3. Propene Formation. To form propene, the adsorbed propoxide species must release a H atom, and the obtained propene then desorbs from the surface.The H atom of propoxide can be abstracted either by the nearby lattice oxygen or by the newly formed OH groups. Following the low-energy pathways in the last section, we have studied the propene formation from the *i*-propoxide species on the O(1) and O(2) sites. Considering that there is a large number of lattice O's available, we have investigated the second CH bond breaking ($C_3H_7 \rightarrow C_3H_6 + H$) on a clean V_2O_5(001) surface starting from an adsorbed

(61) Fu, G.; Xu, X.; Lu, X.; Wan, H. *J. Am. Chem. Soc.* **2005**, *127*, 3989.

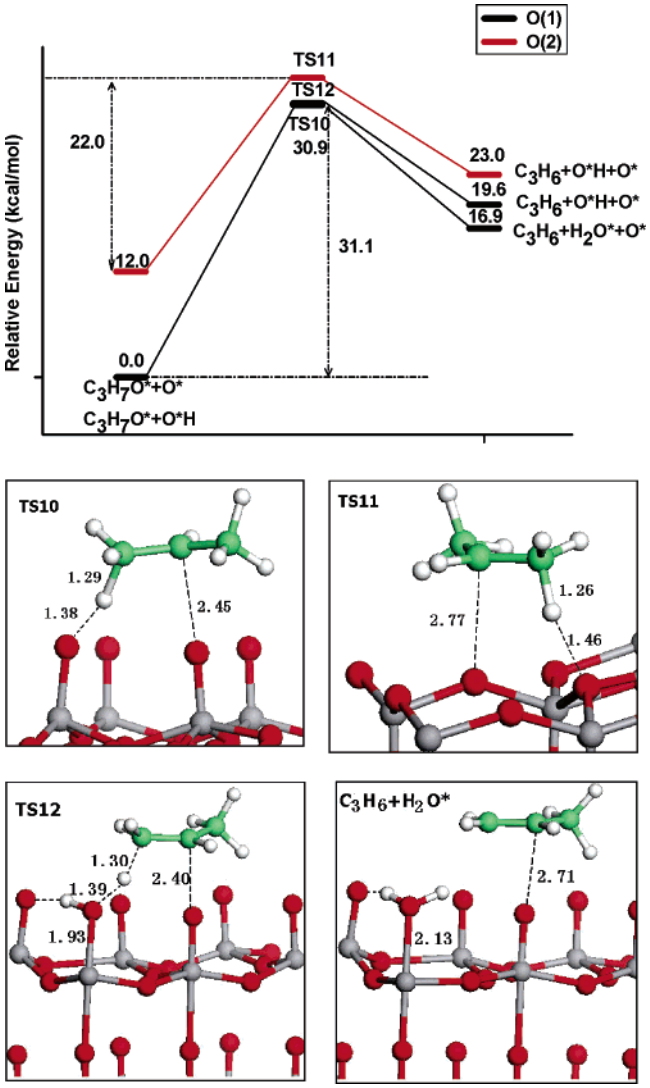

Figure 5. Reaction pathways of propene formation through H abstraction from *i*-propoxide by surface oxygen or surface OH group.

i-propoxide. We noticed that without taking into account the dissociated H in the last step, the difference of adsorption energies of *i*-propoxide at the O(1) and at the O(2) site is 11.7 kcal/mol, which is similar to that in the presence of the H (12.0 kcal/mol). This indicates that this simplified picture can well describe the reactivity between the O(1) and the O(2) site.

Starting from an *i*-propoxide at the O(1) site, we examined three pathways with the H ending up at the nearby O(1), O(2), and O(3) sites. The H atom abstraction by the nearest O(1) atom is the most favored pathway, and the located transition state is shown in Figure 5. The process is endothermic with the reaction energy (the total energy difference between the two states) of 19.6 kcal/mol. The H abstraction is highly activated with a reaction barrier of 30.9 kcal/mol, and the reverse reaction is much easier with $E_a = \sim 11$ kcal/mol. It is concluded that the propene formation from *i*-propoxide species on the O(1) is difficult, both thermodynamically and kinetically.

Alternatively, the H may be abstracted by a nearby hydroxyl group, leading to a water formation simultaneously. Gilardoni et al.[36] found the most favorable pathway of propene formation is through H abstraction by the nearby hydroxyl group on the O(3) site instead of the oxygen. We explored this reaction

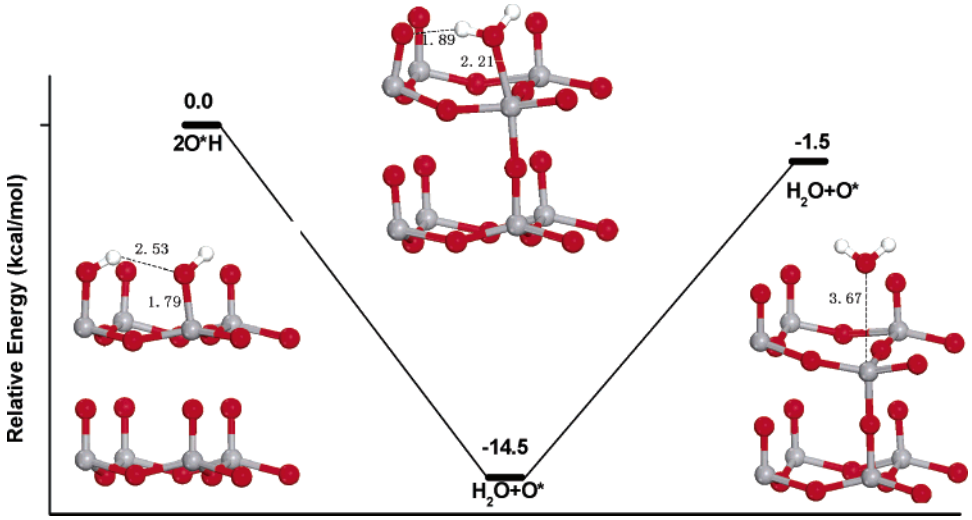

Figure 6. Water formation through recombination of two hydroxyl groups on the surface.

pathway by using a two-layer model of the V_2O_5(001) surface. Also shown in Figure 5 is the process of propene formation from *i*-propoxide on the O(1) site through the H abstraction by a nearby OH group on the O(1) (the final state of the O(1)−O(1)-A pathway). The reaction is endothermic with the reaction energy of 16.9 kcal/mol with E_a being 31.1 kcal/mol. Comparing with the H abstraction by lattice O's, we can conclude that the ability of the H abstraction by lattice O's and surface OH are similar.

Starting from an *i*-propoxide on the O(2) site, the H can similarly migrate to the nearby O(1), O(2), and O(3). The energy profile of the most feasible pathway together with the transition state structures are shown in Figure 5. The H atom can migrate to the nearby O(2) and the O(3) sites with similar reaction barriers of about 22.0 kcal/mol, which is about 8.9 kcal/mol lower than that on the O(1) site. The other possibilities of propene formation through the H abstraction by an OH group can be excluded. The H abstraction by a nearby HO(2) (the final state of the O(2)−O(2)-B pathway Figure 4) is found to be endothermic by 32.2 kcal/mol, which indicates an even larger value for the reaction barrier.

Summarizing the above results, we deduced that the lowest-energy pathway for propene formation takes place at the O(2) site through H abstraction by the nearby lattice O(2) or O(3).

3.4. H_2O Formation. The two H atoms from propane will eventually leave the surface in the form of H_2O. The H_2O is produced through the coupling reaction between two adjacent surface hydroxyl groups. If the OH−OH coupling is not feasible, the catalyst will eventually be poisoned. As the H atom binding with the O(1) site is the strongest compared to that on either the O(2) and O(3) site, the O(1)H−O(1)H coupling is the most likely path from thermodynamics. Here a two-layer V_2O_5(001) slab was utilized to study the O(1)H−O(1)H coupling process. The calculated structures and the energy profile are shown in Figure 6.

At the initial state, the two adjacent hydroxyl groups on O(1) sites tend to form hydrogen bonds. The subsequent proton transfer is exothermic by 14.5 kcal/mol without a reaction barrier. The produced water molecule is very stable on the surface and forms H bonds with nearby O(1) [O(1)−H distance of 1.89 Å, Figure 6]. The H_2O adsorption energy is calculated to be 13.0 kcal/mol. It is noticed that after H_2O desorption, the vanadium atom with an O vacancy relaxes substantially inward to bind with a second-layer O(1) atom.

Furthermore, we also examined the possibility of the O(2)H−O(2)H coupling. The proton-transfer process is endothermic with the reaction energy of 8.0 kcal/mol. This indicates that it is difficult to form water by two O(2)H coupling. Instead, the H on the surface may migrate to the O(1) site first and then form H_2O from there.

4. General Comments on the Mechanism of Propane ODH Reaction

With all the results presented, we summarized the overall energy profiles of the whole propane ODH reaction in Figure 7 where only the most feasible pathways on the O(1) and the O(2) sites are shown. It can be seen clearly that the reaction energy profile over the O(1) site is only 3.1 kcal/mol lower than that over the O(2) site. However, at the O(1) site the propene formation process (E_a = 30.9 kcal/mol) is much more difficult than that at the O(2) site due to the high stability of *i*-propoxide at the O(1).

To fully compare the reaction rate over the O(1) and O(2) site, we have to estimate the effect of the entropy term (exp[$\Delta S/R$]) that affects the preexponential factor in the rate equation. The current DFT methods, however, cannot compute the entropy term accurately (mainly due to the errors in calculating the low-frequency vibrational modes), which is the reason that most computational studies on catalytic reactions did not calculate the term from first principles. Nevertheless, it is known that the preexponential factors for similar types of reactions are rather similar, for example for Eley−Rideal (ER) mechanism reactions, it is around 10^9, and it is around 10^{13} for Langmuir−Hinshelwood (LH) mechanism reactions.[62,63] For the ODH reaction, the first C−H bond breaking belongs to the ER mechanism; therefore, it has a low preexponential factor due to the significant loss of entropy on going from the gas-phase molecule to the TS on the surface. By contrast, the second C−H bond breaking belongs to the LH mechanism. This difference determines that, at 800 K, the first step C−H bond breaking should have a lower reaction rate, even though its reaction

(62) Eichler, A.; Hafner, J. *J. Catal.* **2001**, *204*, 118.
(63) Liu, Z. P.; Hu, P.; Alavi, A. *J. Am. Chem. Soc.* **2002**, *124*, 14770.

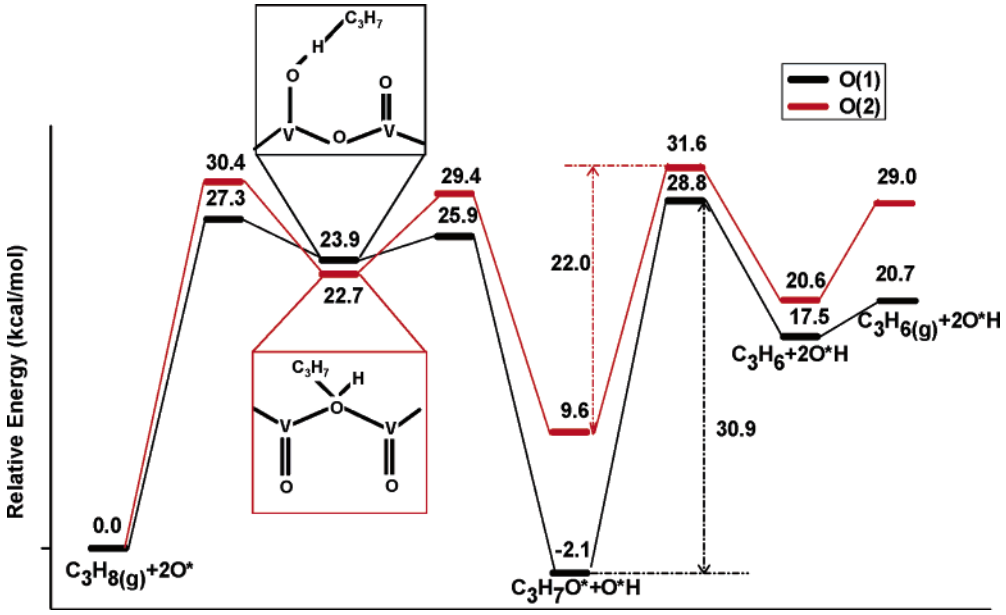

Figure 7. Lowest-energy pathways of propane ODH process occurred on O(1) and O(2), respectively.

barrier is lower than the second C−H bond breaking by 4 kcal/mol. Similarly, considering that the second C−H bond breaking over the O(1) and O(2) site differs by ∼9 kcal/mol in the reaction barrier, it indicates that the difference in the $\exp[-E_a/RT]$ term is more than 0.2×10^3 at 800 K and more than 10^3 at 600 K. Since the second C−H bond breakings at O(1) and O(2) are all surface reactions belonging to the LH mechanism, the preexponential factor difference between them is unlikely to be more than 10^2. Therefore, the second C−H bond breaking at the O(1) site is expected to be slower than that at the O(2) site, particularly, at low temperatures.

Since the initial C−H bond activation is a direct dissociation process, the initial chance of a propane to hit an O(1) and an O(2) is similar to that for hitting V_2O_5(001). Once the C−H is dissociated, the *i*-propoxide species at the O(1) site is slow in further decomposition that leads to the propene formation and desorption, while the *i*-propoxide species at the O(2) site can readily go further to produce propene. As the residency time of the *i*-propoxide at the O(1) site can be rather long, this will open up the side-reaction channels, such as a complete oxidation to undesired CO_x products.[64] Microscopically, it is the O(1) being too active that greatly stabilizes the reaction intermediate. Our result is consistent with the experimental findings,[10] which shows that at high vanadium loading conditions, the selectivity is low.

To us, the most surprising finding in this work is that it is not necessary to have the active terminal V═O species in ODH catalysts. In fact, the presence of the V═O may even lead to side reactions. For a good catalyst, there is a compromise between the activity in C−H bond activation and the easiness to release the propene molecule from the surface. This might be the reason the supported vanadium catalysts are found to be the most efficient in practice. From the experimental point of view, both the basicity of the surface oxygen and reducibility of vanadium atoms can be tuned by varying the polymerization extent of vanadium and modifying the support oxides. From our study, for example, the reducibility of the O(2) site is indeed much facilitated by other surface atoms, which is a rather long-range effect. In supported catalysts, multiple lattice O species are available, including V═O, V−O−V, and V−O−M sites (M is the metal cation from oxide supports). This introduces much flexibility in controlling the catalyst activity as the electronic structures of the two-coordinated O and the terminal V═O in these systems can be very different from the V_2O_5 bulk.

5. Conclusions

In summary, we present a comprehensive survey of the mechanism of oxidative dehydrogenation reaction of propane over various sites on the V_2O_5(001) surface by using periodic DFT methods. Three reaction mechanisms have been explored for the initial C−H bond activation. On the O(1) site, both the radical and oxo-insertion mechanisms are feasible. On the O(2) site, the oxo-insertion mechanism is much more preferred compared to the others. The O(3) site is inert in the C−H bond activation. The calculated reaction barriers of the methylene C−H bond activation are 27.3 and 30.4 kcal/mol on the O(1) and the O(2) sites, respectively. By taking into account the zero-point energy and the thermal energy correction that would increase our calculated values by <4 cal/mol (as mentioned in section 2), our values are a little higher than the experimental value of 24 kcal/mol for ODH reaction occurred on ZrO_2-supported vanadium catalyst.[22] The discrepancy can be partly attributed to the difference between the single-crystal model and the practical supported catalyst. The energy cost to activate a terminal methyl C−H bond in propane is much higher.

The formation of propene from *i*-propoxide on the O(1) site is hindered by high reaction barriers (>30 kcal/mol). Propene can be readily formed through an *i*-propoxide on the O(2) site, releasing a H atom to a nearby O(2) or O(3) atom. The energy barrier is 22.0 kcal/mol. The water formation through the recombination of two surface OH groups at the O(1) site is facile, but the following process of water desorption is endothermic with the reaction energy of 13.0 kcal/mol.

Overall, the vanadyl oxygen O(1) on the V_2O_5(001) surface is slightly more reactive in C−H bond activation than is the O(2) atom. However, the propoxide on the O(2) is much easier

(64) Argyle, M. D.; Chen, K.; Resini, C.; Krebs, C.; Bell, A. T.; Iglesia, E. *J. Phys. Chem. B* **2004**, *108*, 2345.

to further decompose into propene. This provides valuable hints in relating the properties of lattice O to the catalyst activity. For the ODH reaction, the high activities in activating C−H bond and in producing propene are two properties acting negatively to each other. It is expected that the activity of the oxide-supported vanadium can be tuned by controlling the polymerization extent and the support materials.

Acknowledgment. This work was supported by the National Natural Science Foundation of China (Nos. 20433020, 20573023), the National Science Foundation of Shanghai Science and Technology Committee (02DJ14023, 04JC14016, 05DZ22313), National Major basic Research Program of China (Grant No. 2003CB615807), and National High Performance Computing Center of China (No. 00510). We are grateful to the Shanghai supercomputer center and Fudan university supercomputer center for their allocation of computer time.

JA0611745